

Detectability of CMB tensor B modes via delensing with weak lensing galaxy surveys

Laura Marian and Gary M. Bernstein

Department of Physics and Astronomy, University of Pennsylvania, Philadelphia, Pennsylvania 19104, USA

(Dated: July 2, 2007)

We analyze the possibility of delensing Cosmic Microwave Background (CMB) polarization maps using foreground weak lensing (WL) information. We build an estimator of the CMB lensing potential out of optimally combined projected potential estimators to different source redshift bins. Our estimator is most sensitive to the redshift depth of the WL survey, less so to the shape noise level. Estimators built using galaxy surveys like LSST and SNAP recover up to 80-90% of the potential fluctuations power at $l \leq 100$ but only ≈ 10 -20% of the small-angular-scale power ($l \leq 1000$). This translates into a 30-50% reduction in the lensing B -mode power.

We illustrate the potential advantages of a 21-cm survey by considering a fiducial WL survey for which we take the redshift depth z_{max} and the effective angular concentration of sources \bar{n} as free parameters. For a noise level of $1 \mu\text{K arcmin}$ in the polarization map itself, as projected for a CMBPol experiment, and a beam with $\theta_{\text{FWHM}}=10 \text{ arcmin}$, we find that going to $z_{max}=20$ at $\bar{n}=100 \text{ galaxies/arcmin}^2$ yields a delensing performance similar to that of a quadratic lensing potential estimator applied to small-scale CMB maps: the lensing B -mode contamination is reduced by almost an order of magnitude. In this case, there is also a reduction by a factor of ≈ 4 in the detectability threshold of the tensor B -mode power. At this CMB noise level, the B -mode detection threshold is only $3\times$ lower even for perfect delensing, so there is little gain from sources with $z_{max} > 20$. The delensing gains are lost if the CMB beam exceeds $\sim 20 \text{ arcmin}$. The delensing gains and useful z_{max} depend acutely on the CMB map noise level, but beam sizes below 10 arcmin do not help. Delensing via foreground sources does not require arcminute-resolution CMB observations, a substantial practical advantage over the use of CMB observables for delensing.

PACS numbers: 98.62.Sb, 98.80.-k, 98.70.Vc, 98.80.Es

I. INTRODUCTION

The anisotropies in the CMB have been long recognized as a major probe for cosmology. The WMAP satellite has measured the temperature fluctuations up to $l_{max} \leq 1000$ and has confirmed the cosmological standard model of a power-law, flat, ΛCDM universe. Much hope lies with CMB polarization measurements because they have the potential to unveil some of the unknowns of inflation. While some predictions of inflation (such as nearly flat space curvature, nearly scale-invariant power spectrum, and Gaussianity of the primordial fluctuations) have been confirmed by CMB and large scale structure experiments, there is another prediction which is yet to be verified. This is the existence of an almost scale-invariant spectrum of gravitational waves, whose amplitude is directly related to the energy scale of inflation. The inflationary gravitational waves are tensor perturbations to the metric and we expect them to leave a curl-like signature in the CMB polarization field, i.e. a B -mode pattern. Density fluctuations, arising from scalar perturbations to the metric, create a gradient-like component in the polarization field, the E mode. In the linear regime, density fluctuations do not create a B mode, so a detection of the latter would confirm the existence of primordial gravitational waves; it would also provide the energy scale of inflation, which we could use to distinguish between different inflationary scenarios.

CMB polarization measurements are difficult to carry out, primarily for two reasons. Firstly, the amplitude

of the signal is very small: for example, the scalar E -mode power is 2-3 orders of magnitude smaller than the scalar temperature power, tensor B -mode much lower. Secondly, the polarization foregrounds are very poorly understood and they dominate the CMB signal at almost all relevant frequencies. Therefore, foreground removal and detector sensitivity are two of the most stifling limitations of a polarization experiment.

B -mode measurements are additionally obstructed by WL contamination, especially of the recombination signal ($l \leq 100$). Thus CMB polarization measurements are able to provide inflationary insights to the extent to which we can: 1. remove the foreground contribution to the overall signal and 2. delens the B mode power and extract the tensor contribution to it. The delensing process consists of the reconstruction of the lensing potential from chosen observables. The estimated lensing potential is then used to evaluate the WL-created B -mode signal and to subtract it from the measured B -mode map.

In this paper we probe the ability of weak lensing (WL) galaxy surveys to delens the CMB in the absence of foregrounds. To be specific, we try to answer two questions: what attributes should a galaxy or 21 cm WL survey and also a CMB polarization mission have in order to detect the tensor B mode? What is the minimum amplitude of the B mode, expressed in terms of the tensor-to-scalar ratio, r , that can be detected using galaxy or recombination observations for delensing? We take three examples of surveys to illustrate how our estimator works: the ground-based Large Synoptic Survey Telescope (LSST [26]), the space-based Supernova Accel-

eration Probe (SNAP [27]) and a toy model mimicking recombination-era 21-cm observations that we mention in more detail in section §IV. The outline of the paper is as follows. In §II we describe the WL contamination of the tensor B mode. In §III we present our minimum-variance lensing estimator. In §IV we determine the minimum detectable r when we use this estimator to delens. In §V we discuss our results and draw conclusions. Let us now briefly mention similar work existing in the literature. There has been a vast and impressive amount of work on the topic of CMB delensing and r -detection. The great majority of this work uses the CMB observables Θ, E, B to reconstruct the projected potential. Averaging over various quadratic combinations of the temperature field (e.g. see the work of Zaldarriaga and Seljak [1], Bernardeau [2], Hu [3], Hu [4]) and the polarization field (e.g. Guzik et al. [5], Hu and Okamoto [6], Kesden et al. [7]) has been thoroughly considered for the projected potential reconstruction. To give a quick summary: one can build minimum-variance, unbiased estimators, using certain field statistics, as shown by Hu [4]. For a post-Planck experiment (sensitivity of $0.3 \mu\text{K arcmin}$ and beam size of 3 arcmin), Hu and Okamoto [6] found that the most efficient of these estimators can map the potential up to $l \leq 1000$. Kesden et al. [8] and Knox and Song [9] used this last estimator to predict the minimum detectable r as a function of CMB experimental characteristics. There is another, more promising method for lensing potential reconstruction, based on likelihood techniques. Hirata and Seljak [10] have built a maximum-likelihood estimator for the convergence field using temperature maps and have found its performance similar to that of the quadratic estimator introduced by Hu [4]. Hirata and Seljak [11] found that the same maximum likelihood estimator built from polarization maps is even more effective: there is an order of magnitude reduction in the mean squared error in the lensing reconstruction compared to the quadratic estimator method, if the survey characteristics are adequate: sensitivity of $0.25 \mu\text{K arcmin}$ and a beam size of 2 arcmin . Amarie et al. [12] analyze the detectability of tensor B modes in the presence of polarized dust emission, as a function of sky coverage; Verde et al. [13] do a study of optimal surveys for B -mode detection, considering both dust and synchrotron emissions. One disadvantage of the reconstruction methods presented so far is that they require high-resolution CMB maps: they use arc-minute structures of the CMB fields, to reconstruct degree-scale maps of the deflection field, as explained by Hu [4]. Sigurdson and Cooray [14] point out that one can use non-CMB observables to delens the CMB; in this case the requirement for high angular resolution of the CMB mission can be relaxed significantly. These authors determine lower limits for the detectable r using the 21 cm radiation emitted by neutral hydrogen atoms to delens the CMB. We follow a similar approach here, but employ foreground galaxies instead of 21-cm emission as the source plane for delensing.

II. B MODES AND WEAK LENSING

As mentioned in §I, inflation predicts scalar and tensor perturbations; the former are responsible for density fluctuations and for the formation of structure. The latter are gravitational waves. Direct detection of gravitational waves has been a physicists' dream for a long time and there is ongoing effort to make this dream come true (e.g. see LISA [28], LIGO [29]). There is however another means to ascertain the existence of tensor perturbations, by measuring the CMB polarization.

The E and B modes are defined as linear combinations of the Stokes parameters Q and U , such that the power of B arising from linear order *scalar perturbations* is zero, as shown by Zaldarriaga and Seljak [15]. Tensor perturbations yield both E and B modes, roughly of the same magnitude; both modes could in principle provide information on gravitational waves and inflation, but in practice the tensor E modes are overwhelmed by their scalar counterparts. The amplitude of tensor modes is quantified by the tensor-to-scalar ratio r , the ratio of the expectation values for the quadrupole tensor and scalar temperature anisotropies.

Even if one assumes flawless detector technology, B -mode measurements are plagued by the presence of polarized foregrounds and by WL contamination. A detailed discussion of the foreground problem is beyond the scope of this work and we refer the interested reader to the Final Report of the Task Force on CMB Research [16]. We briefly mention that while most galactic polarized foreground emission is currently not well known at the frequencies of interest to CMB experiments, there is reason to believe that this situation will change in the near future. Indeed, the WMAP satellite is gathering all-sky data on the synchrotron emission and the HFI instrument on the Planck satellite will map the dust emission. Numerous smaller, ground-based missions, with higher angular resolution, plan to complement the above-mentioned satellite data. All this information should enable the study of polarized foreground emission as a function of both frequency and angular scale.

We now sketch the equations that describe the WL contamination of the tensor B mode. The groundwork on this subject was done by Zaldarriaga and Seljak [17]; for a more recent review see Lewis and Challinor [18]. A photon travelling from the last scattering surface is affected by potential wells along the line of sight. Its frequency changes because the potentials vary with time (the Rees-Sciama effect, the integrated Sachs-Wolfe effect) and its path can be transversally shifted by lensing. To a good approximation, the lensed wave has the same Stokes parameters along a path \hat{n} as the unlensed one, only shifted by the average deflection along that path:

$$\begin{pmatrix} \tilde{I} \\ \tilde{Q} \\ \tilde{U} \end{pmatrix}(\hat{n}) = \begin{pmatrix} I \\ Q \\ U \end{pmatrix}(\hat{n} + \alpha).$$

where we denote by \tilde{X} the lensed field of parameter X ,

and α is the deflection angle. To linear order, the deflection angle is the gradient of the projected potential: $\alpha = \nabla\psi$. Assuming that deflection angles are very small compared to the characteristic scale of fluctuations, we can Taylor expand the lensed parameters around the undeflected path \hat{x} . Using the flat-sky approximation, we can write the lensed B mode in Fourier space as:

$$\tilde{B}(\mathbf{l}) = B(\mathbf{l}) - \int \frac{d^2l'}{2\pi} f(\mathbf{l}', \mathbf{l}) \psi(\mathbf{l}) E(\mathbf{l}') - \frac{1}{2} \int \frac{d^2l'}{2\pi} \frac{d^2l''}{2\pi} g(\mathbf{l}', \mathbf{l}'', \mathbf{l}) \psi(\mathbf{l}'') \psi^*(\mathbf{l}'' - \mathbf{l}) E(\mathbf{l}'). \quad (2.1)$$

Here B denotes the tensor B mode and E is the unlensed, scalar E mode. The above equation neglects the lensing effect on the tensor E and B fields, since it is very small compared to the lensing of the scalar E mode. The functions f and g are defined by:

$$f(\mathbf{l}', \mathbf{l}) = \mathbf{l}' \cdot \mathbf{l} \sin[2(\phi_{l'} - \phi_l)] \\ g(\mathbf{l}', \mathbf{l}'', \mathbf{l}) = \mathbf{l}' \cdot (\mathbf{l}'' - \mathbf{l}) (\mathbf{l}' \cdot \mathbf{l}'') \sin[2(\phi_{l'} - \phi_l)], \quad (2.2)$$

where $\mathbf{L} = \mathbf{l} - \mathbf{l}'$ and ϕ_l is the angle between \mathbf{l} and the x axis. We assume statistical isotropy and parity invariance and we adopt the power spectrum definition of Lewis and Challinor [18]:

$$\begin{aligned} \langle E(\mathbf{l}) E^*(\mathbf{l}') \rangle &= \delta(\mathbf{l} - \mathbf{l}') C_l^E, \\ \langle B(\mathbf{l}) B^*(\mathbf{l}') \rangle &= \delta(\mathbf{l} - \mathbf{l}') C_l^B, \\ \langle B(\mathbf{l}) E^*(\mathbf{l}') \rangle &= 0. \end{aligned} \quad (2.3)$$

With the above considerations in mind, we write down the lensed B -mode power spectrum as a sum of the tensor (primordial) B -mode power and the weak lensing B -mode power:

$$\tilde{C}_l^B = C_l^B + C_l^{WL}, \quad (2.4)$$

with the appropriate definitions:

$$\begin{aligned} C_l^B &= r C_l^{tensor} \\ C_l^{WL} &= \int \frac{d^2l'}{(2\pi)^2} |f(\mathbf{l}', \mathbf{l})|^2 C_L^\psi C_{l'}^E + \\ &+ \frac{1}{4} \int \frac{d^2l'}{(2\pi)^2} \frac{d^2l''}{(2\pi)^2} |g(\mathbf{l}', \mathbf{l}'', \mathbf{l})|^2 C_{l''}^\psi C_{|\mathbf{l}'' - \mathbf{l}|}^\psi C_{l'}^E, \end{aligned} \quad (2.5)$$

where C_l^B is the tensor B mode power spectrum, C_l^E is the power spectrum of the unlensed scalar E mode and C_l^ψ is the lensing potential power spectrum.

III. THE CMB POTENTIAL ESTIMATOR

A. The ideal case

The measurable B -mode power is a sum of the primordial B -mode tensor power and a convolution in Fourier

space of the scalar E -mode power with the lensing potential power, as shown in Eq. (2.4). In order to have access to the tensor B mode, we need to subtract the lensing contribution from the measured B -mode map. The impediments are that we know neither the lensing potential nor the unlensed E mode power.

In this section we address the first of these problems and build a lensing potential estimator using WL foreground galaxy survey information, independent of a CMB experiment. Unlike the estimators built out of CMB observables, our estimator does not require extremely high resolution in the CMB polarization map. This is an important advantage, since high resolution is the main cost driver of CMB polarization experiments. The disadvantage of our approach is that WL surveys detect source galaxies up to a certain redshift, depending on the specifics of the survey. Our estimator cannot reconstruct the potential fluctuations evolving between that upper-limit redshift and the redshift of recombination.

We build the lensing potential estimator as a weighted sum of the projected potential measured to different source galaxy redshift bins. We choose the weights so that the estimator be optimal, i.e. the variance of the error in each mode is minimal. We work in the flat sky approximation and we assume a flat Friedmann-Robertson-Walker (FRW) metric. We write the estimator as:

$$\hat{\psi}_{\text{CMB}}(\mathbf{l}) = \sum_i \alpha_i(\mathbf{l}) \hat{\psi}_i(\mathbf{l}), \quad (3.1)$$

where the sum is over source bins i and the α_i 's weight the contribution of the projected potential to each redshift source bin. The projected potential to the i th source bin is defined by:

$$\psi_i(\boldsymbol{\theta}) = \int_0^{\chi_\infty} d\chi W_i(\chi) \Phi^{3D}(\chi \boldsymbol{\theta}, \chi), \quad (3.2)$$

where $\Phi^{3D}(\chi \boldsymbol{\theta}, \chi)$ is the 3D gravitational potential spectrum. In Eq. (3.1) we use the Fourier transform of the projected potential: $\psi_i(\mathbf{l}) = \int d^2\theta e^{-i\mathbf{l} \cdot \boldsymbol{\theta}} \psi_i(\boldsymbol{\theta})$. The lensing weight function $W_i(\chi)$ of the source bin i is given by:

$$W_i(\chi) = \frac{2}{c^2} \frac{\int_{z_i}^{z_{i+1}} dz_s \mathcal{P}(z_s) \frac{\chi(z_s) - \chi}{\chi(z_s) \chi} u(z_s - z(\chi))}{\int_{z_i}^{z_{i+1}} dz_s \mathcal{P}(z_s)}. \quad (3.3)$$

Here $u(x)$ is the Heaviside unit step function and $\mathcal{P}(z_s)$ is the redshift distribution of the source galaxies. The residual of our estimator, defined as:

$$\mathcal{R}^\psi(\mathbf{l}) \equiv \psi_{\text{CMB}}(\mathbf{l}) - \hat{\psi}_{\text{CMB}}(\mathbf{l}),$$

tells us how the estimator compares to the true CMB projected potential:

$$\psi_{\text{CMB}}(\boldsymbol{\theta}) = \int_0^{\chi_\infty} d\chi W_{\text{CMB}}(\chi) \Phi^{3D}(\chi \boldsymbol{\theta}, \chi),$$

where $W_{\text{CMB}}(\chi)$ is the same weight as in eq. (3.3), but written for the particular case of one source at redshift z_{CMB} , i.e. $\mathcal{P}(z_s) = \delta_D(z_{\text{CMB}} - z_s)$:

$$W_{\text{CMB}}(\chi) = \frac{2}{c^2} \frac{\chi(z_{\text{CMB}}) - \chi}{\chi(z_{\text{CMB}}) \chi}.$$

We determine the weights α by requiring that the variance of the above-mentioned residual be minimal:

$$\frac{\partial}{\partial \alpha_k(l)} \langle |\psi_{\text{CMB}}(l) - \hat{\psi}_{\text{CMB}}(l)|^2 \rangle = 0, \quad \forall k. \quad (3.4)$$

To see the solution of this equation, let us express the variance of the estimator's residual as a matrix equation:

$$\langle |\psi_{\text{CMB}}(l) - \hat{\psi}_{\text{CMB}}(l)|^2 \rangle = \alpha(l) \cdot \mathcal{W}^{\text{gg}}(l) \cdot \alpha^t(l) - 2\alpha(l) \cdot \mathcal{W}^{\text{gCMB}}(l) + \mathcal{W}^{\text{CMB CMB}}(l). \quad (3.5)$$

In the above equation we have used the following definitions:

$$\begin{aligned} \mathcal{W}_{ij}^{\text{gg}}(l) &\equiv \langle \psi_i(l) \psi_j^*(l) \rangle, \\ \mathcal{W}_i^{\text{gCMB}}(l) &\equiv \langle \psi_i(l) \psi_{\text{CMB}}^*(l) \rangle, \\ \mathcal{W}^{\text{CMB CMB}}(l) &\equiv \langle \psi_{\text{CMB}}(l) \psi_{\text{CMB}}^*(l) \rangle. \end{aligned} \quad (3.6)$$

Using the relation $P_\Phi(k) = [\frac{3}{2} H_0^2 \Omega_m^0 (1+z)]^2 \frac{1}{k^4} P_\delta(k)$, to go from the potential power spectrum to the density power spectrum and also the Limber approximation, we calculate the \mathcal{W} -matrices:

$$\begin{aligned} \mathcal{W}_{ij}^{\text{gg}}(l) &= \frac{\mathcal{W}_0^2}{l^4} \int_0^\infty dz \frac{d\chi}{dz} (1+z)^2 W_i(\chi) W_j(\chi) P_\delta\left(\frac{l}{\chi}\right), \\ \mathcal{W}_i^{\text{gCMB}}(l) &= \frac{\mathcal{W}_0^2}{l^4} \int_0^\infty dz \frac{d\chi}{dz} (1+z)^2 W_i(\chi) W_{\text{CMB}}(\chi) P_\delta\left(\frac{l}{\chi}\right), \\ \mathcal{W}^{\text{CMB CMB}}(l) &= \frac{\mathcal{W}_0^2}{l^4} \int_0^\infty dz \frac{d\chi}{dz} (1+z)^2 W_{\text{CMB}}^2(\chi) P_\delta\left(\frac{l}{\chi}\right), \end{aligned} \quad (3.7)$$

where $\mathcal{W}_0 \equiv 3H_0^2 \Omega_m^0$

We are now able to write down the weights α that minimize the variance of our estimator's residual:

$$\alpha(l) = \mathcal{W}^{\text{gCMB}}(l) \cdot (\mathcal{W}^{\text{gg}})^{-1}(l). \quad (3.8)$$

We note that the weights depend only on the magnitude of l . Our next goal is to rewrite the expression of the variance of $\mathcal{R}(l)$, using eq. (3.8); the l -dependence is implicit here:

$$\text{Var } \mathcal{R}^\psi = \mathcal{W}^{\text{CMB CMB}} - \mathcal{W}^{\text{gCMB}} \cdot (\mathcal{W}^{\text{gg}})^{-1} \cdot \mathcal{W}^{\text{gCMB}}. \quad (3.9)$$

The modes where $\text{Var } \mathcal{R}(l) \rightarrow 0$ are well reconstructed by our estimator.

B. The effect of Shape Noise

So far we have considered an ideal case, with clean WL measurements. In fact we expect the shape noise

of galaxies to limit the performance of our estimator quite significantly. The intrinsic ellipticities of galaxies increase the variance of the projected potential in each source bin. The shape noise effect on $\mathcal{W}^{\text{gg}}(l)$ is:

$$(\mathcal{W}_{ij}^{\text{gg}})_{SN}(l) = \mathcal{W}_{ij}^{\text{gg}}(l) + \frac{\sigma_\gamma^2}{\bar{n}_i} \frac{4}{l^4} \delta_{ij}, \quad (3.10)$$

where σ_γ is the uncertainty in the measurement of one galaxy and \bar{n}_i is the number density of sources in bin i .

C. The CMB Lensing Potential Estimator for Fiducial Surveys

We use three examples of WL surveys to probe the efficiency of our estimator: (i) the ground-based LSST; (ii) the space-based SNAP; (iii) a toy model, which could be a future cosmic 21-cm radiation survey. Depending on the instrument used, four characteristics describe a WL survey: the redshift distribution of the source galaxies, $\mathcal{P}(z)$, the angular concentration of source galaxies, \bar{n} , the area of the sky covered, \mathcal{A} , and the noise level of the intrinsic ellipticities of galaxies, σ_γ . In all cases, we take $\sigma_\gamma = 0.3$. For observations of 21-cm emission at $z > 5$, the lensing signal might be extracted from shape or density correlations of discrete objects (e.g. “minihalos”, Barkana and Loeb [23]) while at higher redshifts the deflection field may be derived from an analysis of the full 3D data cube in a manner analogous to the estimation of lensing from the CMB itself (e.g. Zahn and Zaldarriaga [24]). We retain the notation of σ_γ and \bar{n} even in the absence of discrete sources, since the quantity σ_γ^2/\bar{n} still has meaning as the noise level of the lensing reconstruction. The attainable shape noise levels from 21-cm observations of $z > 5$ are highly dependent on the level of foreground contamination and the history of reionization, so we will retain the simple \bar{n} parameterization in this paper. For LSST and SNAP we employ the source distribution introduced by Smail et al. [19]:

$$\mathcal{P}(z) = \frac{1}{2z_0^3} \exp(-z/z_0). \quad (3.11)$$

We normalize this distribution so that

$$\int_0^\infty dz \mathcal{P}(z) = \bar{n}.$$

The mean redshift of this distribution is $\langle z \rangle = 3z_0$, where z_0 is a survey parameter. For LSST, we take $z_0 = 0.33$, $\bar{n} = 30$ galaxies/arcmin² and $\mathcal{A} = 20000$ deg². For SNAP, $z_0 = 0.5$, $\bar{n} = 100$ galaxies/arcmin² and $\mathcal{A} = 1000$ deg². For the toy model we adopt a “box” (Heaviside) source galaxy distribution, i.e. all source bins have equal number of source galaxies:

$$\mathcal{P}(z) = \mathcal{U}(z_{\text{max}} - z). \quad (3.12)$$

Since we are trying to find an optimal WL survey for our projected potential estimator, we consider z_{max} and \bar{n} as

free parameters for the toy model: z_{max} ranges from 1 to 100 and \bar{n} from 4 to 250 galaxies/arcmin². However, we do fix $\mathcal{A}=20000$ deg², just like for LSST; this seems a reasonable choice, which also allows us to compare the delensing efficiencies of the two surveys.

We now specify a few noise definitions for CMB polarization experiments, which will be relevant in section §IV. We adopt the conventions of Knox [20]. We assume that different pixels in the polarization map have uncorrelated noise with uniform variance σ_{pix}^2 . For one detector, $\sigma_{pix}^2 = \frac{s^2}{t_{pix}}$, where s is the sensitivity of the detector and t_{pix} is the time spent on the pixel. Then the noise power spectrum is:

$$C_l^N \equiv \langle a_{lm}^N a_{l'm'}^{N*} \rangle = w^{-1} (W_l^{beam})^{-2} \delta_{ll'} \delta_{mm'}. \quad (3.13)$$

Here, w is the weight per solid angle, given by: $w^{-1} = \sigma_{pix}^2 \Omega_{pix}$. The weight per solid angle has the advantage that is independent of the beam size for fixed survey time and survey area. We choose the beam to be Gaussian, therefore the beam window function is: $W_l^{beam} = \exp(-l^2 \sigma_{beam}^2/2)$, where $\sigma_{beam}^2 = \theta_{fwhm}^2/8 \ln 2$.

We define a weighted estimator for the measured E mode, with weights chosen so that the variance of the residual of this estimator is minimal. In this case the estimator $\hat{E}(l)$ is just a scalar weight α_l^E times the noisy observation of $E(l)$. Following the same steps as in the case of the lensing potential estimator, the weights and the variance of the residual of the measured E mode estimator are:

$$\begin{aligned} \alpha_l^E &= \frac{C_l^E}{C_l^E + C_l^N}, \\ \text{Var } \mathcal{R}^E(l) &= \frac{C_l^E C_l^N}{C_l^E + C_l^N}. \end{aligned} \quad (3.14)$$

All the results in this paper correspond to a fiducial cosmology in accord with the third year WMAP data release, i.e. Spergel et al. [21]: flat Λ CDM universe with $\Omega_m h^2=0.128$, $\Omega_b h^2=0.02$, $h=0.73$, $n_s=0.96$, $\tau=0.089$ and $\sigma_8=0.76$.

Figure 1 shows the variance of the residual $\mathcal{R}(l)$, scaled by the CMB projected potential power spectrum, for the three examples that we consider. The SNAP (LSST) estimator removes up to 90% (80%) of the CMB projected power for the lowest multipoles ($l \leq 100$) and only up to 20% (10%) for $l \leq 1000$. This happens largely for two reasons. First and most important, LSST and SNAP do not have source galaxies at redshifts higher than ≈ 4 and ≈ 6 , respectively. Therefore the potential fluctuations between the upper-limit redshifts 4(6) and 1100 cannot be reconstructed; since the horizon is much smaller at these redshifts than today, the small scale power suffers greatly from this effect. Second, the shot noise starts to dominate the lensing signal at $l \approx 1000$, so the reconstruction is bound to fail at high multipoles, independent of the cosmological information provided by the source bins. It is easier to separate the impact of shot noise on the estimator from that of the redshift depth of the WL survey

if we look at our third fiducial survey, the box distribution. The green, solid line shows the performance of the optimal estimator using the box distribution with $z_{max}=5$ and $\bar{n}=100$ galaxies/arcmin². The total shot noise is the same as for SNAP, but the reconstruction is improved because there are more high-redshift sources. If we take $z_{max}=20$ and keep the same total angular concentration of galaxies, then the estimator improves by a factor of ≈ 3 at low multipoles. We expect that by taking $z_{max} \rightarrow z_{CMB}$ and $\bar{n} \rightarrow \infty$, we can recover entirely the projected potential to the CMB. The red solid curve in Fig. 1, corresponding to a redshift depth of 100 for the box distribution, seems to confirm this expectation. The estimator's efficiency increases relatively smoothly with the value of \bar{n} : the difference between having 100 and 250 galaxies/arcmin² leads to at most a factor of 2 in the estimator's efficiency for $z_{max}=100$. This difference becomes smaller with lower z_{max} . We conclude that for the purpose of the CMB projected potential reconstruction, going to high redshift in a WL survey is much more important than trying to resolve a high number density of source galaxies. In section §IV we give a more quantitative flavor to this conclusion and discuss what values of \bar{n} and z_{max} we need in a WL survey to significantly delens a B -mode map.

IV. DETECTING THE TENSOR-TO-SCALAR RATIO

A. The Null-Hypothesis Test

We would like to answer the following question: given a CMB survey, how much can we improve the detectability of the tensor-to-scalar ratio r if we use our projected-potential estimator to delens the CMB? There are several factors that influence the answer to this question: the sensitivity and angular resolution of the CMB experiment that measures the B modes, the noise level and redshift depth of the WL survey that provides the information for our potential estimator and, finally, the true value of r itself. The statistical significance of detection for some $r > 0$ is estimated from the χ^2 statistic that would be obtained under the null hypothesis $r = 0$. The underlying approximation is that the delensed B mode obeys Gaussian statistics, which would be true for perfect delensing and no foregrounds. We choose the scenario $r = 0$ to be our fiducial model. We compare other models, with $r \neq 0$ to the fiducial one and we determine the minimum r statistically distinguishable from $r = 0$. The delensed $B^{del}(l)$ will be constructed by subtracting from the lensed $\tilde{B}(l)$ an estimate of the two lensing terms in equation (2.1). Accounting for the fact that we do not have access to the real lensing potential and E mode, but

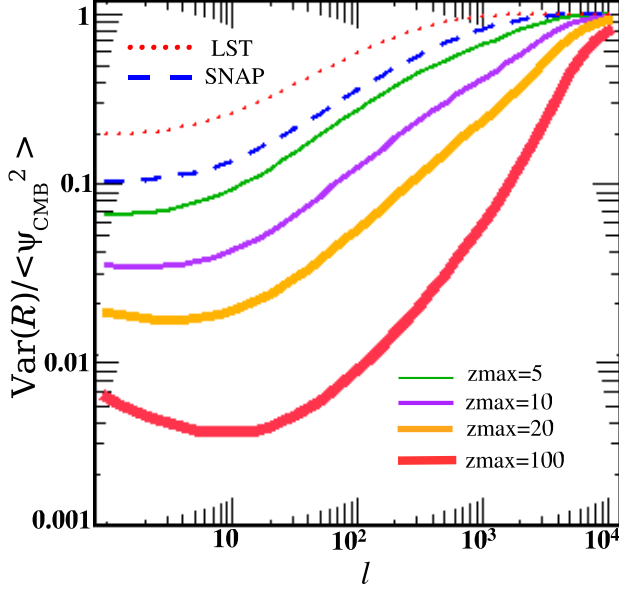


FIG. 1: The residual variance of the CMB lensing potential relative to its original value. LSST is the red dotted line, SNAP is the blue dashed line and the solid lines are for the box distribution. For the latter case, $\bar{n}=100$ galaxies/arcmin² and the thickness of the lines increases with the redshift depth of the survey.

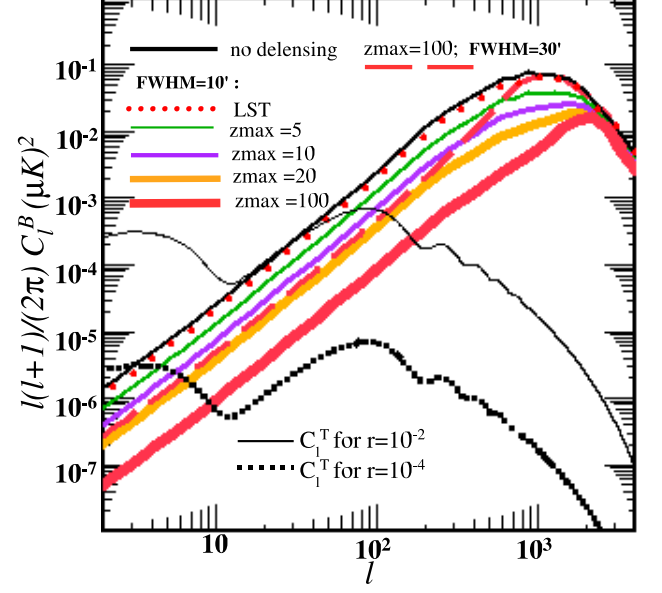


FIG. 2: The power spectra of the tensor B mode, the WL B -mode contamination and its residual after delensing. The black dotted and thin solid lines are the tensor B mode power spectra for $r=10^{-4}$ and $r=10^{-2}$, respectively. The upper solid black line is the full WL B mode power and the rest of the lines are the residual contamination power spectra after delensing with our optimal estimator. The latter correspond to $w^{-1/2}=1\mu\text{K arcmin}$ and $\theta_{\text{FWHM}}=10$ arcmin. The red, long-dashed curve corresponds to $\theta_{\text{FWHM}}=30$ arcmin and $z_{\text{max}}=100$.

their estimators, the delensed field is:

$$B^{\text{del}}(\mathbf{l}) = B(\mathbf{l}) - \int \frac{d^2 l'}{2\pi} f(\mathbf{l}', \mathbf{l}) \left[\psi(\mathbf{L}) E(\mathbf{l}') - \hat{\psi}(\mathbf{L}) \hat{E}(\mathbf{l}') \right] - \frac{1}{2} \int \frac{d^2 l' d^2 l''}{2\pi} g(\mathbf{l}', \mathbf{l}'', \mathbf{l}) \left[\psi(\mathbf{l}'') \psi^*(\mathbf{l}'' - \mathbf{L}) E(\mathbf{l}') - \hat{\psi}(\mathbf{l}'') \hat{\psi}^*(\mathbf{l}'' - \mathbf{L}) \hat{E}(\mathbf{l}') \right] + B^N(\mathbf{l}). \quad (4.1)$$

We include the measurement noise B^N , whose variance is given by equation (3.13). The variance of the measured, delensed B mode follows from the above:

$$C_l^{B, \text{del}} = r C_l^{\text{tensor}} + C_l^N + C_l^{WL, \text{del}}. \quad (4.2)$$

We can express the residual power left from delensing, $C_l^{WL, \text{del}}$, in terms of the variance of the residuals of \hat{E} and $\hat{\psi}$, and the power spectra of the real lensing potential and E mode:

$$C_l^{WL, \text{del}} = \int \frac{d^2 l'}{2\pi} |f(\mathbf{l}', \mathbf{l})|^2 \left[C_L^\psi \text{Var} \mathcal{R}_{l'}^E + \text{Var} \mathcal{R}_L^\psi C_{l'}^E - \text{Var} \mathcal{R}_L^\psi \text{Var} \mathcal{R}_{l'}^E \right] + \frac{1}{4} \int \frac{d^2 l' d^2 l''}{2\pi} |g(\mathbf{l}', \mathbf{l}'', \mathbf{l})|^2 \times \{ C_{l''}^\psi C_{|\mathbf{l}'' - \mathbf{L}|} \text{Var} \mathcal{R}_{l'}^E + (C_{l'}^E - \text{Var} \mathcal{R}_{l'}^E) [C_{l''}^\psi \text{Var} \mathcal{R}_{|\mathbf{l}'' - \mathbf{L}|}^\psi + C_{|\mathbf{l}'' - \mathbf{L}|} \text{Var} \mathcal{R}_{l'}^\psi - \text{Var} \mathcal{R}_{l'}^\psi \text{Var} \mathcal{R}_{|\mathbf{l}'' - \mathbf{L}|}^\psi] \}. \quad (4.3)$$

The last integral in the above equation, containing terms of the second order in the potential power, yields a much smaller contribution to $C_l^{WL, \text{del}}$ compared to the first term. For computational simplicity, we choose therefore to neglect this last term; all the results following have been obtained in this approximation. Let us write the $\Delta\chi^2$ for the measured and delensed B-mode power spectrum:

$$\Delta\chi^2(r) = \sum_l \left[C_l^{B, \text{del}}(r) - C_l^{B, \text{del}}(r=0) \right]^2 \text{Var} \left[C_l^{B, \text{del}}(r) \right]_{r=0}^{-1}. \quad (4.4)$$

The variance of the delensed B-mode power spectrum is:

$$\text{Var}(C_l^{B, \text{del}}(r)) = \frac{2}{(2l+1)f_{\text{sky}}} \left[r C_l^{\text{tensor}} + C_l^N + C_l^{WL, \text{del}} \right]^2. \quad (4.5)$$

Here f_{sky} denotes the fraction of sky covered by the CMB mission. To be able to use our lensing potential estimator, the CMB experiment must survey the same area of the sky as the WL experiment. Using the above equation in the case of the fiducial model $r=0$, we rewrite Eq. (4.4) as:

$$\Delta\chi^2(r) = \sum_l \frac{2l+1}{2} f_{\text{sky}} \left[\frac{r C_l^{\text{tensor}}}{C_l^{WL, \text{del}} + C_l^N} \right]^2. \quad (4.6)$$

In order to find the smallest r discernible from the fiducial value of 0, we need to solve the following equation:

$$\Delta\chi^2(r) = \alpha^2, \quad (4.7)$$

where α sets the confidence level. All our results are computed for $\alpha=2$, which corresponds to a 95% confidence level for a single free parameter r .

B. Results

Figure 2 shows the lensing B mode, given by Eq. 2.6 and the tensor B mode for two values of $r = 10^{-2}, 10^{-4}$. The latter was computed using the publicly available code CAMB, i.e. [30], Lewis et al. [22]. Also shown is the residual lensing power, given by Eq. 4.3, when delensing using LSST and box estimators has been applied. With one exception, the plots correspond to a beam $\theta_{\text{FWHM}}=10$ arcmin; for all of them, the noise level is $w^{-1/2} = 1\mu\text{K arcmin}$, i.e the expected CMBPol noise level.

We can see that LSST delensing can reduce the lensing B -mode power by a factor of ≈ 1.3 (≈ 2 for SNAP, although not shown in the figure), while a box with $z_{\text{max}}=20$ and $\bar{n}=100$ galaxies/arcmin² leaves a residual power ≈ 8 times lower than the original contamination. Although such high redshifts are not attainable by a WL galaxy survey, we would like to illustrate the potential benefits of a 21-cm emission survey. There is further improvement as we go to higher z_{max} : for $z_{\text{max}}=100$ and the same value of \bar{n} , the residual lensing power is ≈ 37 times lower than the full lensing B -mode power. Increasing the beam width has a dramatic effect: the long-dashed red line is for the same box with $z_{\text{max}}=100$, but a beam with $\theta_{\text{FWHM}}=30$ arcmin; compared to the 10 arcmin beam, the delensing efficiency has dropped by a factor of 6. This is understood as follows: the lensed B -mode at $l \sim 10$ –100 arises in part from the beating of E -mode power at $l \sim 1000$ with deflection power at similar l . The delensing must know both these E and deflection fields at $l \approx 1000$ in order to succeed, hence the CMB experiment must resolve these modes.

Naturally, we would like to probe now how much delensing with the above-mentioned WL survey models impacts the detection of tensor modes. In figure 3 we plot the minimum tensor-to-scalar ratio distinguishable from 0 at 95% confidence level as a function of the CMB experimental noise for a fixed beam $\theta_{\text{FWHM}}=10$ arcmin. r_{min} is obtained by solving Eq. 4.7 for some of the delensing scenarios discussed earlier and the noise is in the form of weight per solid angle, $w^{-1/2}$. The upper thin, solid, black curve corresponds to the case when no delensing is done. We also show (turquoise and red arrows) the approximate noise levels $w^{-1/2} = 60$ and $1 \mu\text{K arcmin}$ for two future missions: the Planck satellite [31] and CMBPol. The noise level for the latter was estimated by assuming 1000 detectors with a sensitivity of $50 \mu\text{K}\sqrt{\text{sec}}$, sky coverage of 20000 deg² and 5 years of operation. Delensing is relevant for the detection of

tensor B modes only if the instrumental noise is low enough, $w^{-1/2} < 10\mu\text{K arcmin}$. And this is an optimistic value, since our analysis does not take foregrounds into account. While CMBPol is meant to reach such low noise levels, delensing will not, most probably, be a concern for Planck. This is in accord with the findings of the Planck Science Team. For low noise levels, when delensing does play a part, figure 3 reinforces our earlier conclusions: the difference between the case of no delensing and that of a box distribution going to $z_{\text{max}}=20$ translates approximately into a factor of 7 difference in the corresponding r_{min} for the lowest detector noise that we consider, $w^{-1/2} = 0.1\mu\text{K arcmin}$. $z_{\text{max}}=100$ gains another order of magnitude in the detection threshold of the tensor B modes, for the same weight per solid angle. This is quite idealized, however: for the technically ambitious CMBPol, at $w^{-1/2} = 1\mu\text{K arcmin}$, the extension to $z_{\text{max}}=100$ gains only a factor of 3 over $z_{\text{max}}=20$. The 21-cm signal does not exist significantly above $z \approx 100$ since the hydrogen spin temperature is expected to match the CMB temperature at earlier epochs, for instance see Barkana and Loeb [23] and Zahn and Zaldarriaga [24].

We note that r_{min} corresponding to LSST delensing is lower by a factor of ≈ 3 than the SNAP r_{min} , despite the better performance of the SNAP lensing potential estimator. This is due to LSST's superior sky coverage and the presumed larger CMB sky coverage. We emphasize that the improvement in r_{min} for LSST and SNAP delensing relative to the case of no delensing (corresponding to their respective survey areas of 20000 deg² and 1000 deg²) is of only $\approx 20\%$ and 50% , respectively. We expected this result: the potential modes with angular scales of $l \approx 1000$ mix with E power and generate the low- l B mode polarization power; but such high- l lensing potential modes are poorly reconstructed by both LSST and SNAP.

Figure 4 illustrates the importance of the beam choice for our delensing method. For the CMBPol noise level $w^{-1/2} = 1\mu\text{K arcmin}$, we plot r_{min} as a function of beam size, for the same box models mentioned in Fig. 3. If $\theta_{\text{FWHM}} \leq 10$ arcmin, r_{min} stays constant for all models considered. But once $\theta_{\text{FWHM}} > 10$ arcmin, the delensing efficiency drops steeply and for $\theta_{\text{FWHM}} = 2^\circ$, there is nothing to be gained from delensing.

We now explore the importance of the WL free parameters z_{max} and \bar{n} for the tensor B modes detection. Figure 5 is a contour plot of r_{min} as a function of redshift depth and angular concentration of source galaxies. All contours are plotted using the box distribution for a CMBPol-level of detector noise, $\theta_{\text{FWHM}}=10$ arcmin and a 20000 deg² sky coverage. This plot confirms our findings from section §III C. Once a certain source density is reached ($\bar{n} \approx 50$ galaxies/arcmin² at $z_{\text{max}} \leq 10$), there is no significant improvement in r_{min} if we continue to increase \bar{n} . The redshift depth is the dominant parameter of the WL survey: even with a concentration as low as 10 galaxies/arcmin², if we reach sources at $z=15$, r_{min} has a factor of 2 improvement over the case of no delensing.

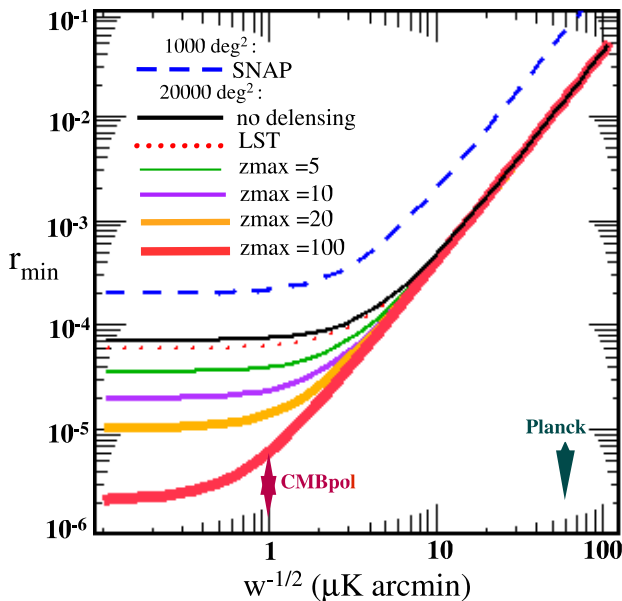


FIG. 3: The minimum tensor-to-scalar r distinguishable from 0 at 95% confidence level as a function of CMB detector noise. All curves are for $\bar{n} = 100$ galaxies/arcmin², with the exception of the LSST line, for which $\bar{n} = 30$ galaxies/arcmin². The upper blue dashed curve is for SNAP delensing ($\mathcal{A} = 1000$ deg²). The rest of the lines correspond to a 20000 deg² sky coverage and match the delensing cases presented in Fig. 2. We have also indicated the approximate polarization noise levels for the Planck and CMBPol missions.

Only if we reach $z_{max} \geq 100$ can we significantly improve r_{min} by increasing \bar{n} above 50 galaxies/arcmin².

C. Related Work in the Literature

Knox and Song [9] investigate the detectability of inflationary gravitational waves using CMB observables to delens. They apply the quadratic estimator of Hu and Okamoto [6] to a CMB polarization experiment and thus reconstruct the lensing potential. They find that for a noise-free CMB map, the lensing B -mode power can be reduced by an order of magnitude, which corresponds to a similar reduction in r_{min} .

Kesden et al. [8] apply the same quadratic estimator to temperature maps and find similar results as Knox and Song [9].

Sigurdson and Cooray [14] reconstruct the lensing potential using the above-mentioned quadratic estimator applied to 21-cm temperature fluctuations. They account for two distinct sources of noise that affect their estimator: the reconstruction noise, and the unreconstructed lensing due to mass between the 21-cm source redshift and the CMB. In the limit where the reconstruction noise dominates, they find that a 21-cm survey, combined with a very sensitive CMB survey, could reduce the detection

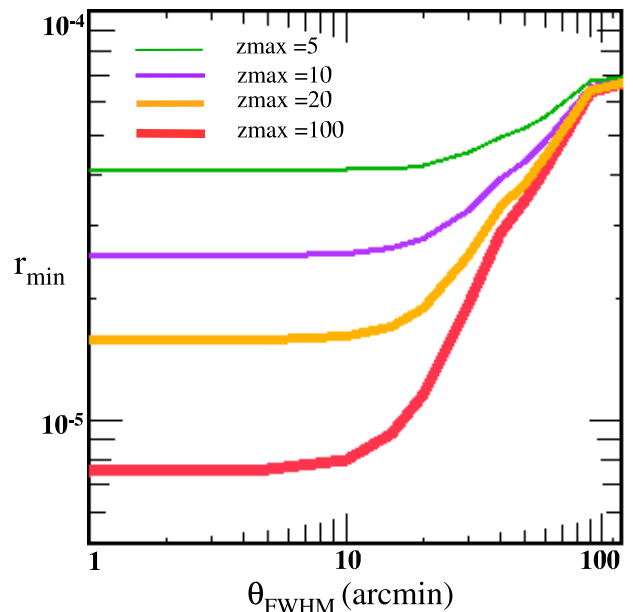


FIG. 4: Dependence of r_{min} on the beam size. The curves are for a box distribution with $z_{max} = 5, 10, 20$ and 100 , $\bar{n} = 100$ galaxies/arcmin² and the noise level of CMBPol.

threshold of the tensor B -mode power by an order of magnitude, compared to the no delensing case. The authors also consider the limit where the partial delensing bias dominates. In this limit, the reduction in the lensing contamination power is the same as what we find if we take $\bar{n} \rightarrow \infty$.

Seljak and Hirata [25] show that the reconstruction of the lensing potential using the maximum likelihood estimator applied to polarization maps can reduce the power of the lensing B mode by at least a factor of 40. They conclude that delensing is not a fundamental limit to the detection of inflationary gravitational waves, if high-resolution CMB maps cleaned of foreground emission are available.

V. CONCLUSIONS

In this paper we have examined the possibility of delensing B -mode polarization maps using galaxy WL surveys. We have proposed a weighted combination of projected potential estimators to different source redshift bins which optimally reconstructs the projected potential seen by the CMB. We have used three fiducial surveys to exemplify our estimator: LSST, SNAP and a generic survey relevant mostly to future 21-cm studies.

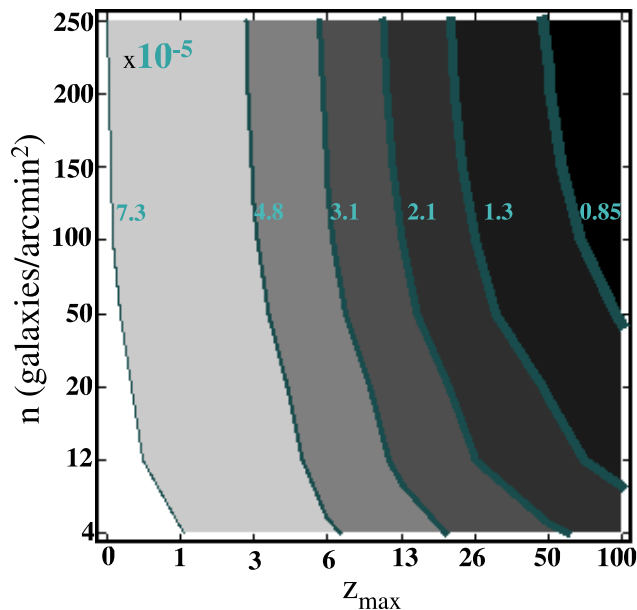


FIG. 5: r_{min} as a function of the WL survey parameters, z_{max} and \bar{n} . The contours are for a box distribution, the noise level of CMBPol and $\theta_{FWHM}=10$ arcmin. Their increasing thickness depicts the change in the detectable tensor B mode amplitude as we transit from a weak delensing case ($z_{max}=1$, $\bar{n}=250$ galaxies/arcmin²) to very good delensing ($z_{max}=100$, $\bar{n}=250$ galaxies/arcmin²).

These examples have different source redshift distribution, source density \bar{n} , and sky coverage f_{sky} , and have enabled us to test the effect of each of these factors on the lensing potential estimator and also on its ability to reduce the WL contamination of B mode maps. Using a $\Delta\chi^2$ test for the delensed B mode field, we have determined the minimum value of the tensor-to-scalar ratio statistically distinguishable from 0 in optimally delensed data. Throughout this paper we have ignored the polarized foreground contamination and we have also made the assumption of Gaussianity for the delensed B mode map. While this assumption may be inaccurate, especially for the cases when the efficiency of delensing is low, we expect the qualitative results of our work to hold.

The lensing potential estimator is sensitive mostly to the redshift depth of the WL survey and reconstructs best the large angular scale multipoles. The performance of the estimator improves continually as higher redshift source galaxies are used. In the limit $z_{max} \rightarrow z_{CMB}$ and $\bar{n} \rightarrow \infty$, the reconstruction is perfect. An experiment like SNAP recovers $\approx 90\%$ of the CMB projected potential power for $l \leq 100$ and $\approx 20\%$ for $l \leq 1000$. The performance of LSST is a little worse, because it detects sources at an average redshift of $\langle z \rangle = 1$, compared to $\langle z \rangle = 1.5$ of SNAP. A box distribution (constant redshift distribution of source galaxies), provides better CMB potential estimator: if we go as far as $z_{max}=20$, there is an order of magnitude improvement over SNAP, for the same angu-

lar concentration of galaxies.

However, in this last case, the reduction in r_{min} , compared to the case where no delensing is done, is only of a factor of ≈ 7 for $w^{-1/2} = 0.1 \mu K$ arcmin and $\theta_{FWHM}=10$ arcmin. This happens because low- l lensing B -modes are generated by beating of gravitational potential modes and E -modes on scales corresponding to $l \approx 1000$, where the potential estimator is less faithful. In the case of LSST and SNAP, the reduction in r_{min} relative to the no delensing case is only by $\approx 15\%$ and $\approx 50\%$ for the same CMB noise level and beam.

We stress that delensing with foreground weak lensing offers significant gains in r_{min} (factors of 5 or more) only when three conditions are met:

1. the noise in the CMB map is sufficiently low, $\sim 1 \mu K$ arcmin;
2. the beam size of the CMB map is < 20 arcmin;
3. the lensing source distribution extends to $z \sim 20$ or greater.

Delensing is not relevant to tensor mode detection if $w^{-1/2} > 10 \mu K$ arcmin or if $\theta_{FWHM} \geq 2^\circ$. Also, there is no advantage in lowering the beam size beyond $\theta_{FWHM}=10$ arcmin: for our delensing method, a 1 arcmin beam will do just as well as a 10 arcmin beam. This is perhaps the most important feature of our delensing technique, as both the quadratic estimator of Hu [4] and the maximum likelihood estimator proposed by Hirata and Seljak [11] require beam sizes of 2-3 arcmin to yield their best performance. For the CMBPol mission, (which might reach a noise of $1 \mu K$ arcmin) delensing with a box of $z_{max}=20$ results in $r_{min} \approx 2 \times 10^{-5}$. If no delensing is applied, then $r_{min} \approx 8 \times 10^{-5}$, a factor of 4 worse. CMBPol detector noise keeps $r_{min} > 7 \times 10^{-6}$ even with perfect delensing, so there is less incentive to acquire delensing source planes above $z_{max}=20$. Also for the CMBPol noise level, we have investigated the impact of \bar{n} and have concluded that as long as we go to high redshift ($z_{max} > 10$), even with a low density of source galaxies, we can still improve r_{min} by a factor of a few.

Acknowledgments

LM is supported by grant BEFS-04-0014-0018 from NASA. GMB acknowledges additional support from Department of Energy grant DOE-DE-FG02-95ER40893 and National Science Foundation grant AST-0607667. This work has substantially benefitted from the suggestions of the anonymous referee: we would like to thank him or her. We are very grateful to Robert E. Smith and Jacek Guzik for their participation in the CMB lensing review sessions. We thank Carlos Hernandez-Monteagudo, Jeff Klein, Dan Swetz and Chris Semisch for useful discussions.

-
- [1] M. Zaldarriaga and U. Seljak, Phys. Rev. D **59**, 123507 (1999), astro-ph/9810257.
 - [2] F. Bernardeau, Astron. Astrophys. **338**, 767 (1998), astro-ph/9802243.
 - [3] W. Hu, Phys. Rev. D **64**, 083005 (2001), astro-ph/0105117.
 - [4] W. Hu, Astrophys. J. Lett. **557**, L79 (2001), astro-ph/0105424.
 - [5] J. Guzik, U. Seljak, and M. Zaldarriaga, Phys. Rev. D **62**, 043517 (2000), astro-ph/9912505.
 - [6] W. Hu and T. Okamoto, Astrophys. J. **574**, 566 (2002), astro-ph/0111606.
 - [7] M. Kesden, A. Cooray, and M. Kamionkowski, Phys. Rev. D **67**, 123507 (2003), astro-ph/0302536.
 - [8] M. Kesden, A. Cooray, and M. Kamionkowski, Physical Review Letters **89**, 011304 (2002), astro-ph/0202434.
 - [9] L. Knox and Y.-S. Song, Physical Review Letters **89**, 011303 (2002), astro-ph/0202286.
 - [10] C. M. Hirata and U. Seljak, Phys. Rev. D **67**, 043001 (2003), astro-ph/0209489.
 - [11] C. M. Hirata and U. Seljak, Phys. Rev. D **68**, 083002 (2003), astro-ph/0306354.
 - [12] M. Amarie, C. Hirata, and U. Seljak, Phys. Rev. D **72**, 123006 (2005), astro-ph/0508293.
 - [13] L. Verde, H. V. Peiris, and R. Jimenez, Journal of Cosmology and Astro-Particle Physics **1**, 19 (2006), astro-ph/0506036.
 - [14] K. Sigurdson and A. Cooray, Physical Review Letters **95**, 211303 (2005), astro-ph/0502549.
 - [15] M. Zaldarriaga and U. Seljak, Phys. Rev. D **55**, 1830 (1997), astro-ph/9609170.
 - [16] J. Bock, S. Church, M. Devlin, G. Hinshaw, A. Lange, A. Lee, L. Page, B. Partridge, J. Ruhl, M. Tegmark, et al., ArXiv Astrophysics e-prints (2006), astro-ph/0604101.
 - [17] M. Zaldarriaga and U. Seljak, Phys. Rev. D **58**, 023003 (1998), astro-ph/9803150.
 - [18] A. Lewis and A. Challinor, Phys. Rep. **429**, 1 (2006), astro-ph/0601594.
 - [19] I. Smail, D. W. Hogg, L. Yan, and J. G. Cohen, Astrophys. J. Lett. **449**, L105+ (1995), arXiv:astro-ph/9506095.
 - [20] L. Knox, Phys. Rev. D **52**, 4307 (1995), astro-ph/9504054.
 - [21] D. N. Spergel, R. Bean, O. Doré, M. R. Nolta, C. L. Bennett, J. Dunkley, G. Hinshaw, N. Jarosik, E. Komatsu, L. Page, et al., Astrophys. J. Supp. **170**, 377 (2007), arXiv:astro-ph/0603449.
 - [22] A. Lewis, A. Challinor, and A. Lasenby, Astrophys. J. **538**, 473 (2000), arXiv:astro-ph/9911177.
 - [23] R. Barkana and A. Loeb, Reports of Progress in Physics **70**, 627 (2007), arXiv:astro-ph/0611541.
 - [24] O. Zahn and M. Zaldarriaga, Astrophys. J. **653**, 922 (2006), astro-ph/0511547.
 - [25] U. Seljak and C. M. Hirata, Phys. Rev. D **69**, 043005 (2004), astro-ph/0310163.
 - [26] <http://www.lsst.org/>
 - [27] <http://snap.lbl.gov/>
 - [28] <http://lisa.nasa.gov/>
 - [29] <http://www.ligo.caltech.edu/>
 - [30] <http://camb.info/>
 - [31] <http://www.rssd.esa.int/Planck>